The Journal of Chemical Physics

Simulation of the CO_2 hydrate–water interfacial energy: The mold integration–guest methodology

Cite as: J. Chem. Phys. **157**, 134709 (2022); https://doi.org/10.1063/5.0101746
Submitted: 03 June 2022 • Accepted: 13 September 2022 • Accepted Manuscript Online: 13 September 2022 • Published Online: 07 October 2022

Iván M. Zerón, José Manuel Míguez, Bruno Mendiboure, et al.

The Journal of Chemical Physics ARTICLE scitation.org/journal/jcp

Simulation of the CO_2 hydrate–water interfacial energy: The mold integration–guest methodology

Cite as: J. Chem. Phys. **157**, 134709 (2022); doi: 10.1063/5.0101746
Submitted: 3 June 2022 • Accepted: 13 September 2022 •
Published Online: 7 October 2022

Iván M. Zerón,[1] José Manuel Míguez,[1] Bruno Mendiboure,[2] Jesús Algaba,[1] and Felipe J. Blas[1,a)]

AFFILIATIONS

[1] Laboratorio de Simulación Molecular y Química Computacional, CIQSO-Centro de Investigación en Química Sostenible and Departamento de Ciencias Integradas, Universidad de Huelva, 21006 Huelva, Spain
[2] Laboratoire des Fluides Complexes et Leurs Réserviors, UMR5150, Université de Pau et des Pays de l'Adour, B.P. 1155, Pau Cdex 64014, France

Note: This paper is part of the JCP Special Topic on Fluids Meets Solids.
[a)] **Author to whom correspondence should be addressed:** felipe@uhu.es

ABSTRACT

The growth pattern and nucleation rate of carbon dioxide hydrate critically depend on the precise value of the hydrate–water interfacial free energy. There exist in the literature only two independent experimental measurements of this thermodynamic magnitude: one obtained by Uchida *et al.* [J. Phys. Chem. B **106**, 8202 (2002)], 28(6) mJ/m^2, and the other by Anderson and co-workers [J. Phys. Chem. B **107**, 3507 (2003)], 30(3) mJ/m^2. Recently, Algaba *et al.* [J. Colloid Interface Sci. **623**, 354 (2022)] have extended the mold integration method proposed by Espinosa and co-workers [J. Chem. Phys. **141**, 134709 (2014)] to deal with the CO_2 hydrate–water interfacial free energy (mold integration–guest or MI-H). Computer simulations predict a value of 29(2) mJ/m^2, in excellent agreement with experimental data. The method is based on the use of a mold of attractive wells located at the crystallographic positions of the oxygen atoms of water molecules in equilibrium hydrate structures to induce the formation of a thin hydrate slab in the liquid phase at coexistence conditions. We propose here a new implementation of the mold integration technique using a mold of attractive wells located now at the crystallographic positions of the carbon atoms of the CO_2 molecules in the equilibrium hydrate structure. We find that the new mold integration–guest methodology, which does not introduce positional or orientational information of the water molecules in the hydrate phase, is able to induce the formation of CO_2 hydrates in an efficient way. More importantly, this new version of the method predicts a CO_2 hydrate–water interfacial energy value of 30(2) mJ/m^2, in excellent agreement with experimental data, which is also fully consistent with the results obtained using the previous methodology.

I. INTRODUCTION

Natural gas hydrates are ice-like compounds in which guest molecules, such as methane (CH_4) or carbon dioxide (CO_2), are enclathrated in the voids left by a periodic hydrogen-bond network of water molecules (host).[1] The guests generally do not compete with the specific interactions (hydrogen bonding in the case of hydrates) that keep together the coordinated lattice formed by the host. Hydrates crystallize in the well-known structures sI, sII, and sH. Hydrates of small molecules, such as CH_4, CO_2, and H_2, form sI hydrates,[1] whereas larger substances, such as C_3H_8, C_4H_{10}, usually form sII and sH hydrate structures that can accommodate heavier organic molecules in the presence of small-sized gases.[1–3]

Fundamental and applied research on hydrates and clathrates has been motivated by several reasons. From an applied point of view, hydrates are potential alternative sources of energy since huge amounts of CH_4 have been identified in hydrate deposits, either on the sea floor or in permafrost frozen substrates.[4,5] In addition to energetic reasons, hydrates also play an important role in flow assurance as gas pipelines are mostly laid in deep seas and oceans. This environment provides favorable thermodynamic conditions for hydrate growth due to the high pressures and low temperatures present. According to this, blockages inside pipelines due to the formation of hydrates provoke important economic impacts and environmental damages.[1,6] Another remarkably relevant aspect of hydrates from both the scientific point of view and practical interest is the possibility to capture[7,8] gas and use them as gas storage and transportation devices.[9–11]

From a more general and fundamental point of view, the microscopic mechanisms that control the thermodynamics, growth

kinetics, and nucleation of these materials are still poorly understood and are far from being satisfactory.[1,12] The microscopic mechanism that allows the formation of a solid phase from its liquid is usually known as nucleation.[12] Crystal nucleation rate and the shape and speed with which solids grow are critically controlled by the interfacial free energy existing at the interface between the emerging crystal and the bulk fluid. In this work, we concentrate on the calculation of the CO_2 hydrate–water interfacial free energy.

Contrary to what happens with the experimental determination of fluid–fluid interfacial tensions, for which well-established and accurate techniques exist in the literature, there is a rather limited number of methods for obtaining experimental solid–fluid (SF) free energy values, and many of them are specific to special solids or situations.[13,14] Solid phases have an infinitely large viscosity, making the methods used to evaluate fluid–fluid interfacial tensions not applicable, although some exceptions can be found in the literature. Particularly, bulk flow can occur with some metals near their melting point. In such cases, solids may act as viscous liquids in which the strain rate is proportional to the applied stress.[15] However, this is not the case for water and hydrates, for which few experimental measures of the solid–fluid interfacial energy exist. Additionally, this magnitude depends on the orientation of the crystal with respect to the fluid, i.e., it is an anisotropic property. As a consequence of this, there exist considerable discrepancies in experimental results. For example, in the case of the ice Ih–water interfacial free energy at atmospheric pressure, its value ranges from 25 to 35 mJ/m^2 depending on the method used to measure it. This represents a wide range of values compared with the established and accepted value of 72 mJ/m^2 for the interfacial tension of liquid water at ambient conditions.[16]

To the best of our knowledge, only two experimental results accounting for the CO_2 hydrate–water interfacial free energy have been published in the literature. Uchida *et al.*[17,18] and Anderson *et al.*[19,20] have (indirectly) measured the interfacial energy of this system using porous media and the Gibbs–Thomson relationship. They found two similar values, 28(6) and 30(3) mJ/m^2, respectively. Other authors have also studied the effect of different porous media at the equilibrium pressure of several hydrates,[21–27] and more recently, Zarifi *et al.*[28] used the same procedure to obtain the interfacial free energy of hydrates of CH_4. It is interesting to mention here the recent work of Phan *et al.*[29] in which the authors measure and estimate the cyclopentane hydrate–water interfacial energy from experiments and computer simulation, respectively.

Clearly, computer simulations of realistic models constitute a valuable and efficient alternative method that can also improve our understanding of the hydrate–water interface from a molecular perspective.[30,31] Although a number of simulation methodologies to calculate SF interfacial free energies exists in the literature,[32–35] all of them are usually efficient for simple molecular models and not all of them are accurate, simple, and cheap from the point of view of computational cost for complex solid structures. Espinosa *et al.*[36] have proposed a novel computer simulation technique called Mold Integration (MI) method to calculate crystal–fluid interfacial free energy from a fundamental point of view. This methodology uses potential energy wells located at the equilibrium crystallographic positions to induce the formation of a crystal slab in the fluid at coexistence conditions. Its reliability was validated first in the original paper with the hard-sphere and Lennard-Jones systems and later for different water models, such as TIP4P, TIP4P/2005, TIP4P/Ice, and mW.[16] It is somehow surprising that the number of studies dealing with the hydrate–water interfacial free energies, including simulation studies, is rather small.[37]

During the last few years, several authors have determined the dissociation line of the CO_2 hydrates using computer simulation, including Míguez *et al.*,[38] as well as Contandy *et al.*[39] and Waage *et al.*,[40] but none of them have obtained its interfacial free energy. More recently, Algaba *et al.*[41] have presented an extension of the MI methodology to deal with the interfacial free energy of the CO_2 hydrate–water interface. They used the TIP4P/Ice model of Abascal *et al.*[42] for describing water and the TraPPE model of Potoff and Siepmann[43] to deal with carbon dioxide. The unlike intermolecular interactions used are the same as those used by Míguez *et al.*[38] The novel implementation of the method is based on the thermodynamic definition of the interfacial free energy, as in the original technique, and on the use of a new selection of the standard local-order parameters to distinguish liquid-like and hydrate-like water molecules during the simulation. The extension of this method and its implementation takes into account several issues not considered in the original MI methodology proposed by Espinosa *et al.*: (1) CO_2 hydrates constitute a binary mixture formed by two components, viz., water, and CO_2, the first component acting as a host molecule and the second one as a guest molecule in the hydrate; (2) for the evaluation of the interfacial energy, it is necessary to explicitly simulate the coexistence of three phases in equilibrium instead two (hydrate, aqueous solution of CO_2 and fluid carbon dioxide); and (3) the traditional election of the rotationally local bond order parameters of Lechner and Dellago[44] needs to be optimized in order to correctly identify liquid-like and hydrate-like water molecules during the simulations.

The extension of the MI technique to deal with CO_2 hydrates, a system formed by two different species (water and CO_2), involves making a decision about the type of mold of attractive sites that is used to induce reversibly the formation of the hydrate slab. Algaba *et al.*[41] opted to use a mold for water molecules, i.e., a mold of attractive interaction sites located in the aqueous solution of CO_2 phase. These sites occupy the equilibrium crystallographic positions of the oxygen atoms of water molecules in one of the principal planes of the sI hydrate structure. This is possibly the simplest and most conservative choice since it follows directly the unique possible election used in the work by Espinosa *et al.* (they used pure water as the liquid phase). It is also the simplest solution since the composition of water in the aqueous solution of carbon dioxide is large compared with that of CO_2 in the solution ($x_{H_2O} \approx 0.94$ and $x_{CO_2} \approx 0.06$ at typical conditions at which dissociation of the CO_2 hydrate takes place). Finally, the use of a mold for water molecules provides microscopic information to the system about the long-range positional and orientational order of water molecules in the sI hydrate structure that facilitates the formation of the hydrate. *A priori*, these reasons make the induction of the hydrate growth from the aqueous phase a successful activation process. Because the mold used by Algaba *et al.* induces the formation of the hydrate by promoting the host molecules (water) to occupy the crystallographic equilibrium position of oxygen atoms of water in the hydrate structure, they called the extension of the method mold integration–host or simply MI-H.[41]

In this work, we follow a more challenging route. Instead of using a mold of interacting sites located at the crystallographic positions of the oxygen atoms of water molecules in the sI hydrate structure, we use a mold of interacting sites located at the crystallographic positions of the carbon atoms of the CO_2 molecules. We call this implementation the mold integration–guest or simply MI-G methodology. It is important to recall here that the cubic sI structure of CO_2 hydrates belongs to the $Pm\bar{3}n$ space group of symmetry and is formed by two types of primitive cages: dodecahedral primitive cages (5^{12}, D) and tetrakaidekahedral primitive cages ($5^{12}6^2$, T). In particular, the unit cell of the sI structure consists of two D cages and six T cages. According to the literature,[1] the CO_2 hydrate exhibits single occupancy in each cage in such a way that each unit cell formed from 46 molecules can accommodate eight CO_2 molecules. The choice of using a mold for CO_2 molecules is in principle more attractive mainly due to two reasons: (1) Coordinates of the mold are easy to identify since they are located at the center of the T and D cages of the sI hydrate structure; and (2) the number of crystallographic positions that have to be specified is lower than in the case of the MI-H method since the CO_2 hydrate is formed from 46 H_2O molecules and 8 CO_2 molecules in each unit cell. However, there is an important question in the air. Is it possible to induce the formation of the hydrate equilibrium structure using this alternative method? This technique provides structural information for the equilibrium positions of the CO_2 in the hydrate but no information on the crystalline structure of water molecules. Will the water molecules in the aqueous solution phase be able to rearrange around the CO_2 molecules, occupy their true equilibrium positions, and with the appropriate order to allow the hydrate to grow consistently?

The main goal of this work is to evaluate the CO_2 hydrate–water interfacial free energy using an extension of the MI methodology with a mold of interacting sites located at the crystallographic positions of the CO_2 molecules in the hydrate structure. To achieve this challenging objective, we need to solve and answer three main questions: (1) Can a mold of associating sites located at the crystallographic positions of the CO_2 molecules in the hydrate induce the formation of a complete sI hydrate structure? (2) If the answer to question (1) is affirmative, is this new methodology able to predict accurately the experimental interfacial energy of the CO_2 hydrate obtained by Uchida, Anderson, and co-workers? (3) Finally, are the predictions obtained from the calculation of the MI-G technique and molecular dynamics (MD) computer simulation consistent with the results obtained by Algaba *et al.*[41] using the MI-H technique? To this end, we use the same realistic water and CO_2 molecular models used previously by Míguez *et al.*[38] and Algaba *et al.*[41] in combination with the new MI-G technique proposed in this work.

It is relevant to mention in this context the work of Radhakrishnan and Trout.[45] These authors proposed the well-known Local Structuring Hypothesis that provides a plausible explanation of the nucleation mechanism of hydrates as an alternative to the also well-known Labile Cluster Hypothesis formulated by Sloan and co-workers.[1] According to Radhakrishnan and Trout,[45] nucleation of CO_2 hydrates takes place as follows: An arrangement of the CO_2 molecules in a configuration similar to that in the equilibrium positions of the guest molecules in the sI structure of the hydrate is produced in the aqueous solution of CO_2 due to a thermal fluctuation. This provokes a new rearrangement, now of water molecules, in a configuration that energetically favors the formation of hydrates. If the number of CO_2 molecules exceeds a certain value, then a critical nucleus of hydrate is formed and nucleation takes place. Several years ago, Hirai and co-workers[46] performed MD simulations of aqueous solutions of CO_2 fixing guest molecules at all of the equilibrium positions of the guest molecules in the sI structure of hydrates. This result is directly related to the work of Radhakrishnan and Trout[45] and also to the current study. Hirai *et al.*[46] nicely showed how the water molecules organized themselves into a CO_2 hydrate during the simulations. Particularly clear and relevant to this work are the snapshots presented by these authors in Figs. 3 and 4 25 years ago.[46] From this perspective, it will be highly interesting to check if the same behavior is observed during the simulations presented in this work using the new version of the MI technique.

The organization of this paper is as follows: In Sec. II, we introduce the new MI-G methodology used in this work. Molecular simulation details are described in Sec. III. Section IV contains the results obtained in this work, as well as their discussion. Finally, conclusions are presented in Sec. V.

II. METHODOLOGY

The microscopic mechanism that allows the formation of a solid phase from its liquid is usually known as nucleation.[12] When a stable liquid phase is cooled below the temperature at which the solid–fluid (SF) phase transition takes place at a given pressure, also known as the freezing point, it is expected to freeze. However, it is extremely unlikely that nucleation occurs spontaneously. Only if an external driving force exists—such as the presence of impurities, the existence of an interface or a solid substrate, supersaturation/supercooling thermodynamic conditions, or any other mechanism that accelerates the dynamics of the system—nucleation may be observed.[12] The formation of a solid phase in the absence of any of these driving forces is called homogeneous nucleation.[12]

Under thermodynamic conditions of metastability, in which bulk metastable liquids can exist below the freezing point (at a given pressure), small nuclei of the solid phase may be formed due to the existing thermal fluctuations in the system. The formation of these small nuclei constitutes an activated process controlled by two opposite energetic contributions: (1) the degree of metastability of the system, which favors the nucleation, and (2) surface energy that exists due to the presence of interfaces between the metastable bulk liquid and the incipient and small solid nuclei in formation. This implies that nucleation does not occur instantaneously. The picture described in the previous sentences corresponds to the well-known classical nucleation theory (CNT) that allows the description of nucleation in a nice and simple way and prediction of the corresponding free energy barriers from a number of approximations.[12] Crystal nucleation rate and the shape and speed with which solids grow are critically controlled by the interfacial free energy existing at the interface between the emerging crystal and the bulk fluid.

According to the previous discussion, homogeneous nucleation of any crystalline solid phase from its liquid, including hydrates, is an activated process.[12,36,47] The time and length scales of nucleation depend on subcooling, i.e., the difference between the working temperature and the melting temperature of the system. At high

subcooling, the time and length scales at which nucleation occurs are of the order of nanoseconds and nanometers, respectively.[1,12] This is why homogeneous nucleation is considered a rare event, which means that it is nearly impossible to observe spontaneously the growth of a solid phase from its liquid, experimentally or by means of molecular simulation.[1,12]

To overcome this problem and induce the formation of a hydrate solid phase, we place attractive interaction sites in the H_2O-rich liquid phase at the equilibrium positions of certain atoms of the sI structure of the CO_2 hydrate. As we have already mentioned in the Introduction, in our previous work, we use attractive sites at the equilibrium positions of the oxygen atoms of water in the structure of the hydrate.[41] This corresponds to the MI-H version introduced by some of us in a previous study.[41] In this work, however, we extend the MI technique and use a mold of associating sites or wells for the carbon atoms of the CO_2 molecules. In other words, instead of inducing the formation of a hydrate slab forcing the water molecules to occupy their equilibrium positions, we force the guest molecules of the hydrate, i.e., the CO_2 molecules, to occupy their equilibrium positions. According to this, the set of associating sites used to induce the formation of the solid phase corresponds to a mold with coordinates located in the middle of the large (T) and small (D) cages of the sI hydrate structure. Due to this and to differentiate from the original MI and the MI-H versions, we call this extension the Mold Integration–Guest (MI-G) methodology. As we will show later in the paper, the presence of attractive wells of CO_2 molecules is able to induce the appropriate positional and orientational order of water molecules and, consequently, the formation of a thin hydrate slab inside the aqueous solution of CO_2. According to this, the MI-G technique also allows the determination of the interfacial free energy of the CO_2 hydrate.[36,41]

The work needed to form a thin crystal slab of hydrate in the aqueous solution, ΔG^{hw}, is proportional to the hydrate–water interfacial free energy, γ_{hw},

$$\Delta G^{hw} = 2\mathscr{A}\gamma_{hw}, \tag{1}$$

where $\mathscr{A}$ is the cross-section area of the simulation box perpendicular to the direction in which the hydrate grows. Factor 2 appears because two hydrate–water interfaces are formed inside the aqueous solution of CO_2.

The attractive well potential between wells and guest particles in the MI-G technique, U_{wg}, is modeled using the same continuous version of the intermolecular potential proposed by Espinosa *et al.* in the original MI method,[36]

$$U_{wg} = -\frac{1}{2}\varepsilon\left[1 - \tanh\left(\frac{r - r_w}{\alpha}\right)\right]. \tag{2}$$

Here, r is the distance between the well center and the nearby guest molecule, α represents the steepness at the well width, r_w is the distance at which the attractive force is maximum, and ε is the well depth that represents the strength of the attractive well. Following the original work of Espinosa and co-workers,[36] we use here $\alpha = 0.017$ Å. The advantage of this version of the square-well intermolecular potential is that it is a simple and continuously differentiable function. In addition to that, forces between the attractive wells and carbon atoms of the CO_2 molecules are also continuous and well defined and can be used in molecular dynamics simulations. The particular values of r_w and ε critically determine the interfacial free energy values provided by the methodology, as we will in the following sections.

The difference in free energy between the system with the potential well switched off (wells not occupied) and switched on (wells fully occupied), ΔG_m, can be obtained by means of thermodynamic integration along a path in which attraction of the potential wells is gradually switched from $\varepsilon = 0$ to ε_m,

$$\Delta G_m = -\int_0^{\varepsilon_m} \left\langle N_{fw}(\varepsilon)\right\rangle_{NP_z\mathscr{A}T} d\varepsilon. \tag{3}$$

Here, ε_m represents the maximum value of the depth of the wells. According to Espinosa *et al.*, when $\varepsilon = \varepsilon_m$, all the attractive interacting sites must be occupied by carbon atoms of the CO_2 molecules. The function N_{fw} describes the total number of guest molecules trapped by the mold throughout the simulation and $\left\langle N_{fw}(\varepsilon)\right\rangle_{NP_z\mathscr{A}T}$ is the ensemble average occupancy at constant temperature, pressure, and interfacial area. This function typically shows a minimum occupancy when $\varepsilon \to 0$, grows softly as ε increases, and finally $N_{fw}(\varepsilon) \to N_w$ as $\varepsilon \to \varepsilon_m$, indicating that all the potential wells are occupied by carbon atoms of the CO_2 molecules. It is important to recall here that integration of Eq. (3) must be reversible, i.e., the system cannot go through a phase transition. As discussed in the following sections, the election of appropriate values of r_w allows this condition to be fulfilled.

To obtain the reversible work only due to the formation of the crystal slab, i.e., ΔG^{hw}, $-N_w\varepsilon$ is subtracted from free energy changes in the perturbed system due to the extra energy supplied to the system, i.e.,

$$\Delta G^{hw} = \Delta G_m + N_w\varepsilon_m. \tag{4}$$

Here, N_w is the total number of wells implemented in the mold. Now, using Eqs. (1), (3), and (4), one can obtain the CO_2 hydrate–water interfacial free energy.

According to the work of Espinosa *et al.*[36] and Algaba *et al.*,[41] the MI method consists of several steps: (1) preparation of the initial molecular simulation box; (2) determination of the optimal well radius r_w^0; (3) calculation of γ_{hw} for different well radii, below the optimal value, using thermodynamic integration; and (4) extrapolation of γ_{hw} to r_w^0. All the steps are presented and discussed in the Results section.

III. SIMULATION DETAILS

We determine the CO_2 hydrate–water interfacial free energy using the well-known TIP4P/Ice[42] and TraPPE[43] models for water and CO_2, respectively. The intermolecular potential parameters, including the H_2O–CO_2 unlike dispersive energy value, are those presented by Míguez *et al.*[38] Particularly, these molecular models and parameters are the same as those used in our previous calculation of the CO_2 hydrate–water interfacial energy.[41] This election allows us to predict accurately the three-phase hydrate–water–carbon dioxide coexistence or dissociation line of the CO_2 hydrate (see Fig. 10 and Table II of the work of Míguez and co-workers for further details). All simulations are performed at 40 MPa and 287 K. These conditions correspond to a state point of the phase diagram of the water–carbon dioxide binary mixture at

the dissociation line of the CO_2 hydrate, i.e., a point at which the CO_2 hydrate, aqueous solution of CO_2, and the CO_2-rich liquid phase coexist.

We perform MD simulations in combination with the direct coexistence technique in the isothermal–isobaric or $NP_z\mathscr{A}T$ ensemble.[48,49] We use a parallelepiped simulation box of volume $V = L_x \times L_y \times L_z$, where L_x, L_y, and L_z are the dimensions of the simulation box. L_x and L_y are kept constant and only L_z is varied along the simulation. This ensures that the system is under the equilibrium normal pressure (perpendicular to the hydrate slab formed when the mold is switched on). To avoid stress in the slab of the CO_2 hydrate when the mold is switched on, we first simulate a bulk solid phase at the coexistence conditions (287 K and 40 MPa) using the standard NPT ensemble in which the three simulation box sides are allowed to fluctuate independently. The equilibrium L_x and L_y dimensions of the simulation box obtained at 40 MPa, consistent with the equilibrium unit cell of the hydrate phase at coexistence conditions, are then used in the $NP_z\mathscr{A}T$ simulations. This strategy allows the simulation of a non-stressed solid at the equilibrium pressure.[50–52]

We use a Verlet leapfrog algorithm[53] with a time step of 0.002 ns to solve Newton's equations. All simulations are run at constant temperature and pressure using a Nosé–Hoover thermostat[54] and an anisotropic Parrinello–Rahman barostat.[55] The relaxation time used in the thermostat and barostat is 2 and 1 ps, respectively. Long-range interactions due to electrostatic interactions are determined using the Particle Mesh Ewald technique.[56] We use a cutoff radius for both dispersive interactions and the real part of electrostatic interactions of 10 Å. Note that this cutoff distance is the same as that used in our previous studies[38,41] and will allow us to compare the results obtained with full consistency.

IV. RESULTS AND DISCUSSION

In this section, we present the results obtained following the steps of the MI-G methodology: preparation of the initial simulation box in which the CO_2-rich and H_2O-rich liquid phases coexist at 40 MPa and 287 K; election of the mold structure (number of wells and layers); determination of the optimal value of the potential range, $r_w^{(0)}$, at which the interfacial free energy must be evaluated; calculation of the interfacial free energy at different well radius values, r_w, below the optimal potential range value, $r_w^{(0)}$, using reversible thermodynamic integration; and finally, extrapolation of the different values obtained in the previous step to $r_w^{(0)}$.

A. Preparation of the initial simulation box

To prepare the initial simulation box used in this work, we first consider two independent homogeneous liquid systems, a pure water liquid phase formed by 736 molecules of water and two pure CO_2 liquid phases formed by 128 CO_2 molecules each of them. Dimensions of the initial simulation boxes are chosen to be consistent with the size of the hydrate unit cell along the x- and y-axes that will be formed when the mold is switched on. According to this, $L_x = L_y = 24.0374$ Å and they will kept fixed during all the simulations. After this, the final simulation box is built linking up the three bulk boxes forming a CO_2-rich liquid–H_2O-rich liquid–CO_2-rich liquid system. The liquid–liquid (LL) system is equilibrated along 5 ns. After this, the equilibrium value of the length of the simulation box along the z-axis was $L_z \approx 66.5$ Å.

We also place $N_w = 16$ attractive interacting sites at the equilibrium positions of the carbon atoms of CO_2 located at the center of the large and small cages along two principal and parallel planes of the sI structure of the CO_2 hydrate. Particularly, we consider 12 wells in the T (large) cages and 4 wells in the D (small) cages, distributed in two parallel planes inserted in the middle of the simulation box. Figure 1 shows a snapshot of the equilibrated CO_2-rich liquid–H_2O-rich liquid–CO_2-rich liquid simulation box at 287 K and 40 MPa according to the explanation in the previous paragraph. This initial setup is consistent with the configurations used to obtain the dissociation line of the CO_2 hydrate by Míguez *et al.*[57] as well as with those used by Algaba *et al.*[41] to determine the interfacial energy of the CO_2 hydrate–water interface using the MI-H methodology. The mold of the associating wells can be seen in the middle of the simulation box (magenta spheres in a van der Waals representation of the wells for CO_2 molecules). Note that this fluid–fluid box is used during the present work as an initial configuration to perform all the calculations when the mold is switched on. In other words, when the mold is switched off, the system exhibits liquid–liquid immiscibility, and when the mold is switched on, the system develops a thin CO_2 hydrate slab if the parameters of associating wells are appropriate.

The mold used in this work is congruent with a simulation box of the sI hydrate structure formed by a unit cell replicated twice along each direction, i.e., eight unit cells arranged as $2 \times 2 \times 2$ (see Sec. IV B for further details). It is important to mention that finite-size effects could play an important role in the interfacial free energy of the CO_2 hydrate, especially taking into account that capillary fluctuations far from two unit cells could be probably suppressed. These effects are currently under study and will be the subject of a future publication. We also recommend the reader to inspect Fig. 1 of the work of Míguez *et al.*[38] to see the particular positions of the carbon atoms of CO_2 at which the mold sites are placed. Note that according to the original work of Espinosa and co-workers,[36] it is possible to apply the MI methodology using molds composed of a single or two layers (bilayer mold). In this work, we have tried different options of molds. We have opted for a bilayer mold with $N_w = 16$ attractive interacting sites it is the mold with

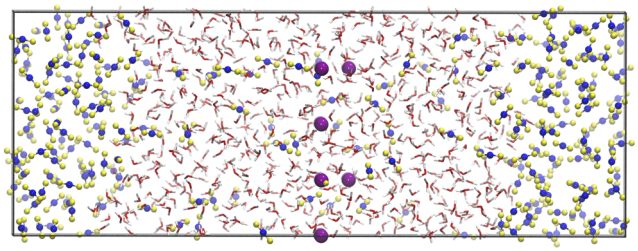

FIG. 1. Snapshot extracted from MD trajectories of a simulation of the water–CO_2 two-phase coexistence at 40 MPa and 287 K obtained with the mold of wells for CO_2 molecules switched off. Red and white licorice representation correspond to oxygen and hydrogen atoms of water, respectively, blue and yellow spheres (van der Waals representation) correspond to carbon and oxygen atoms of CO_2, respectively, and magenta spheres (van der Waals representation) correspond to the mold attractive sites with $r_w = 0.665$ Å and $\varepsilon = 0$.

the minimum number of wells able to induce the formation of a CO_2 hydrate slab in the water phase. The particular options explored in this work are explained in Sec. IV B. Note that the sites are switched off during the setup of the simulation box. They are only switched on when the MI-G method is used, as explained in Sec. IV B.

B. Election of the mold structure

Before determining the appropriate values of r_w and ε, the well radius and the maximum value of the wells, respectively, that allow a calculation of the CO_2 hydrate–water interfacial free energy, it is essential to check that there exists a mold structure able to induce the formation of a CO_2 hydrate slab inside an aqueous solution of CO_2. In the MI-G extension of the MI methodology, the molds are prepared to be occupied by the guest molecules, i.e., CO_2 molecules, particularly, the carbon atoms of these molecules. Note that in the MI-H version of the method, the mold associating wells are prepared to interact only with the oxygen atoms of the water molecules in the aqueous solution.

As mentioned previously, the cubic sI structure of CO_2 hydrates ($Pm\bar{3}n$ space group) is formed by two types of primitive cages: dodecahedral primitive cages (5^{12}, D) and tetrakaidekahedral primitive cages ($5^{12}6^2$, T). Particularly, the unit cell of the sI structure consists of two D cages and six T cages. The D and T cages are the smallest among the five primitive cages that form sI, sII, and sH hydrate structures and both of them can accommodate CO_2 inside, among other small guest molecules.[1] According to this and taking into account that CO_2 hydrates show single occupancy of CO_2 molecules in the cages,[38] a unit cell can be occupied by eight CO_2 molecules. Consequently, in the context of the MI-G methodology, a unit cell can fit up to eight associating sites for the mold.

Let us consider the z-axis direction perpendicular to the hydrate crystalline slab to be induced by the attractive sites of the mold when it is switched on. The size of the initial simulation box along the x- and y-axes is chosen to be consistent with the size of the unit cell of the sI structure. Particularly, L_x and L_y are approximately twice the lattice parameter of the unit cell, a = 12.0187 Å. If we only consider one unit cell along the z-axis direction of the simulation box, it is possible to have one to four layers of molds perpendicular to the z-axis direction, with 12, 4, 12, and 4 associating wells in the first, second, third, and fourth layer, respectively. Choosing the number and the particular combination of layers, it is possible to have a number of wells switched on between 4 and 32. A detailed account of the available layers and the total number of potential site wells is provided in Table I.

In summary, for the case of molds formed from four unit cells of the hydrate sI structure ($2 \times 2 \times 1$ along the $x-$, $y-$, and $z-$axes directions, respectively), the MI-G methodology allows the utilization of *a priori* eight different combinations of layers, with different numbers of associating wells, to induce the formation of a solid slab in the aqueous solution at coexistence. However, the number of layers and the total number of activated associating wells strongly affect the efficiency of the technique, and not all the distributions are appropriate to be used in the MI methodology. According to the original work of Espinosa and co-workers,[58] also followed by Algaba *et al.*,[41] the selected distribution, with all the well sites switched on, must accomplish three key conditions: (1) For low values of the well radius, r_w, the mold must induce the formation of a crystal hydrate at the beginning of all simulations without which induction period, i.e., the size of the hydrate has to grow monotonically, and eventually, occupy the whole simulation box; (2) for high values of the well radius, the switched on mold should not be able to induce the formation of a hydrate that occupies the complete simulation box but only a thin slab of hydrate; and finally, (3) there must exist at least one large r_w, according to condition (2), for which all the positions of the mold are occupied by only one molecule (in this particular case, by only one CO_2 molecule). According to this, we have chosen $\varepsilon = 12k_BT$, and r_w = 0.760, and 1.267 Å as the low and high values of the well radius. With r_w = 0.633 Å, molds formed by 4, 8, and 12 sites are not able to induce the formation of a complete hydrate. In addition to that, using r_w = 1.267 Å molds with 20, 24, 28, and 32 sites are not able to induce the formation of thin slabs of hydrates. However, the distribution of sites (1100) accomplishes the three conditions previously mentioned.

TABLE I. Distribution of the layers and associating sites of the mold in the MI-G methodology according to N_s, the total number of wells activated, N_L, the number of layers used to induce the formation of a CO_2 hydrate slab, and the structure of layers that have sites switched on. Nomenclature (1010) means that the first and third layers are switched on and the second and fourth are switched off.

N_s	N_L	Structure of layers
4	1	(0100)
8	2	(0101)
12	1	(1000)
16	2	(1100)
20	3	(0111)
24	2	(1010)
28	3	(1110)
32	4	(1111)

Figure 2 shows two snapshots corresponding to the x–y and y–z projections of the simulation box in which appears the mold used in this work. Particularly, the mold corresponds to the (1100) structure of layers presented in Table I. The x–y projection of the simulation box shows the N_w = 16 associating well chosen. Note that the 16 wells, as we have mentioned previously, are located in two different layers: one containing 12 wells and the other containing 4 wells. Although this is not clearly seen in the top snapshot of the figure due to the projection, in the bottom snapshot showing the y–z projection of the simulation box, one can distinguish the two layers—the left one containing 12 wells and the right one with 4 wells.

At this point, a key question still remains without an answer. Is it possible to induce the correct formation of the CO_2 hydrate equilibrium structure with the MI-G methodology? We have demonstrated, using the MI-H technique, that a mold of associating wells located in a principal plane, with the wells occupying the crystallographic equilibrium positions of the sI hydrate structure, is able to induce the formation of the CO_2 hydrate.[41] In other words, when the mold of the MI-H method is switched on, (1) the water molecules close to the mold plane occupy the positions of the wells, forming the seed that helps the hydrate to nucleate, (2) the CO_2 molecules in the aqueous solution and additional CO_2 molecules

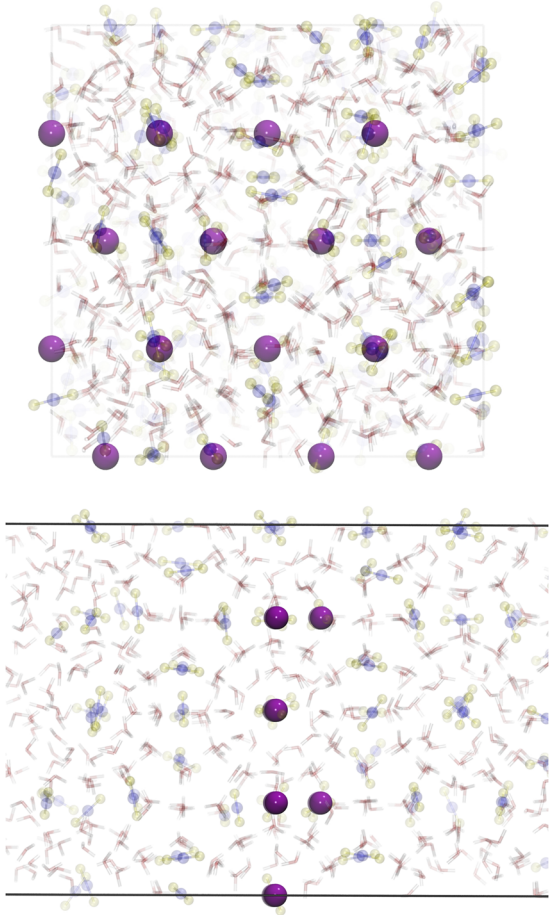

FIG. 2. *x–y* (top) and *y–z* (bottom) projections of the simulation box showing the structure of the mold used in the MI-G methodology. The snapshot has been extracted from MD trajectories showing the crystallization of the CO_2 hydrate using $r_w = 0.665$ Å and $\varepsilon = 12k_BT$, and the same thermodynamic conditions and representations for the molecules as in Fig. 1.

necessary to accomplish the 46:8 water–CO_2 equilibrium proportion per unit cell diffuse (coming from the borders of the simulation box) and move around the seminal layer of water molecules occupying the mold positions, and (3) water molecules in the liquid phase are able to organize themselves in hydrate cages with the CO_2 molecules occupying the inner positions. Depending on the particular values of r_w and ε used, a thin hydrate slab or a complete hydrate phase occupying the whole simulation box is formed. Movies obtained from MD simulations of our previous work[41] included in the supplementary material provide additional evidence on how the MI-H technique works. Particularly, we have included two movies: (1) one using a r_w larger than the optimal value r_w^0, which only allows the induction of a thin slab of CO_2 hydrate, and (2) another with $r_w < r_w^0$, in which the hydrate eventually grows and occupies the whole aqueous phase.

However, in the MI-G method, the situation is not as simple as in the MI-H technique. The mold of wells in this extension only provides structural information for the equilibrium positions of the CO_2 in the hydrate but no information on the crystalline structure of the water molecules. Are the water molecules able to rearrange around the CO_2 molecules, occupy their true equilibrium positions, and with the appropriate orientational order to allow the CO_2 hydrate to grow consistently? Figure 3 shows a snapshot extracted from MD trajectories of a simulation prepared as explained in Sec. IV A with the mold for CO_2 switched on, with $r_w = 0.665$ Å and $\varepsilon = 12k_BT$. As can be seen, under these conditions, the MI-G methodology is able to induce the formation of a hydrate phase that occupies the whole simulation box. It is important to mention that the configurations generated using these values are never considered during the evaluation of the interfacial free energy of the hydrate. These configurations are only presented here to demonstrate that the mold used in this work is able to induce a CO_2 hydrate that eventually grows and occupies nearly the whole simulation box using the MI-G methodology. It will be clear in Sec. IV C that the r_w value of the mold used here is not appropriate to calculate interfacial energies. We have also included in the supplementary material a movie showing how the final configuration shown in the figure is obtained from MD simulation of the system using the r_w and ε parameters, which confirms that the MI-G technique is able to induce the formation of CO_2 hydrates using only as structural information the coordinates of the centers of the cages that form sI hydrates and not the crystallographic positions of the oxygen atoms of the water molecules.

These results, including the snapshot shown in Fig. 3 as well as the movie corresponding to the crystallization of the hydrate using the MI-G presented in the supplementary material, are in agreement with the seminal predictions presented 25 years ago by Hirai and co-workers.[46] Consequently, an arrangement or induction of the CO_2 molecules to occupy the crystallographic positions in the sI structure promotes the formation of hydrates.

Note that here we use $\varepsilon_m = 12k_BT$ instead of the $8k_BT$ value used originally by Espinosa *et al.*[16] and by some of us in our previous work.[41] In a first stage of the research, we used $\varepsilon_m = 8k_BT$. Unfortunately, with this value, the mold does not get a full occupancy of the wells. See below the behavior of the average number of filled wells as a function of the well depth ε. We think this is due to the small number of wells used in the mold to accommodate CO_2 molecules

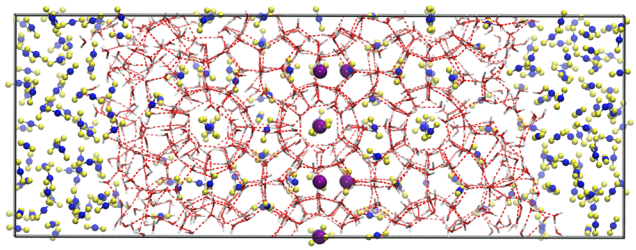

FIG. 3. Snapshot extracted from MD trajectories of a simulation of the water–CO_2 two-phase coexistence at 40 MPa and 287 K obtained with the mold of wells for CO_2 molecules switched on. Red and white licorice representation corresponds to oxygen and hydrogen atoms of water, respectively, blue and yellow spheres (van der Waals representation) correspond to carbon and oxygen atoms of CO_2, respectively, and magenta spheres (van der Waals representation) correspond to the mold attractive sites with $r_w = 0.665$ Å and $\varepsilon = \varepsilon_m = 12k_BT$.

($N_w = 16$). According to this, we use in this work $\varepsilon_m = 12k_BT$, which allows us to get a full occupation of the wells when $\varepsilon \to \varepsilon_m$.

C. Determination of r_w^0

Once we have checked that the selected structure of the mold is able to induce the formation of a solid slab inside the aqueous solution of CO_2, we calculate the optimal well radius r_w^0. According to Espinosa *et al.*[16] and Algaba *et al.*,[41] r_w^0 is determined following the evolution of the number of water molecules that form the crystal slab induced by the model, n_h, as a function of time.

Algaba *et al.*[41] have shown that rotational invariant local bond order parameters constitute a good choice to distinguish between fluid-like and solid-like particles in hydrate systems, such as those proposed by Lechner and Dellago.[44] Particularly, the combination of the local bond order parameters $\bar{q}_3$ and $\bar{q}_6$ is appropriate to discriminate between solid-like and liquid-like water molecules in systems including solid phases that exhibit sI hydrate structures. These order parameters are similar to the translational and orientational order parameters proposed by Truskett *et al.*[59] and Chau and Hardwick,[60] respectively. This approach or similar techniques have been previously used by several authors in the literature to identify if a molecule is a fluid-like or solid-like particle.[16,47,61–64] Here, we follow our previous work[41] and use a $\bar{q}_3 - \bar{q}_6$ representation and a threshold value $\bar{q}_{3,i} \approx 0.038$ to distinguish between water molecules in liquid and hydrate phases. Details of the parameters used to characterize the $\bar{q}_3 - \bar{q}_6$ representation for hydrates can be found in Fig. 3 of the work of Algaba *et al.*[41]

The key point to determine the optimal well radius r_w^0 is what Espinosa *et al.*[16,36] call the induction period. According to their seminal work, the induction period is a time interval that can be observed from the beginning of a simulation starting from a fluid configuration, at $t = 0$ ns, up to a certain time at which n_h starts to grow, on average, monotonically. The time at which the number of water molecules in the solid phase starts to increase depends on the particular value used for r_w. If there does not exist an induction period, the hydrate crystalline slab grows irreversibly with time, i.e., $n_h = n_h(t)$ behaves as an increasing function of time from $t \approx 0$ ns. This indicates that there is no free energy barrier between the fluid and the incipient solid slab. According to this, the formation of the hydrate slab takes place spontaneously. In this case, the radius of the mold used to induce the formation of the slab, r_w, should be below r_w^0, i.e., $r_w < r_w^0$. If there does exist an induction period, $n_h = n_h(t)$ fluctuates around its initial value from $t \approx 0$ ns up to a certain time. Again, the time at which n_h starts to increase with time depends on the r_w value. If r_w is high enough, n_h should behave as a constant function, on average, as we will see later. In this case, this behavior is associated with the existence of a free energy barrier between the fluid and the incipient crystalline slab. This barrier avoids the formation of the crystal slab during a given time. In this case, the radius of the mold used, r_w, is above r_w^0, i.e., $r_w > r_w^0$.

From a practical point of view, r_w^0 is calculated by performing computer simulations in the $NP_z\mathscr{A}T$ ensemble using different r_w values and the initial fluid configuration and the mold structure explained fully switched on ($\varepsilon = \varepsilon_m$). Although the definition of induction period is clear from a thermodynamic point of view, the application of the concept explained in the previous paragraph is subtle. To identify if the r_w values used during a simulation are above or below the optimal value, r_w^0, it is necessary to obtain a statistical picture of the behavior of $n_h = n_h(t)$, especially when r_w values are "close" to those of r_w^0 or when $r_w \sim r_w^0$. To this end, for each r_w value considered, we perform five independent simulations to obtain five different trajectories, each of them showing its own evolution of n_h, the number of water molecules in the induced crystalline hydrate slab, as a function of time. As mentioned in the Introduction, the determination of the interfacial free energy of a hydrate, using the MI-H methodology as well as its extension the MI-G technique, requires longer simulation times compared with other systems, as it occurs in the case of the Ih ice–water interface. In the case of hydrates, the initial configuration used to determine the optimal radius r_w^0 is not a single fluid phase but a two-phase coexisting system. It is important to recall here that the interfacial free energy must be evaluated at coexisting conditions. In the case of the CO_2 hydrate–water interface, it involves the coexistence of three phases (dissociation line).

The two-phase system mentioned in the previous paragraph, the $H_2O + CO_2$ binary mixture, exhibits liquid–liquid immiscibility along the dissociation line of the CO_2 hydrate. The existence of two immiscible phases introduces two important issues in the method that should be taken into account appropriately. The first one is the limited solubility of CO_2 in water. This constitutes a thermodynamic hindrance since the number of CO_2 molecules dissolved in the H_2O-rich liquid phases is not enough to induce the formation of a crystalline hydrate slab when the mold is switched on. In fact, the slab is formed when CO_2 molecules coming from the CO_2-rich liquid phase located at the borders of the simulation box diffuse to the center of the box where the mold is located. This second limitation is controlled by a kinetic hindrance due to the diffusion of CO_2, from the reservoirs located at both extremes of the simulation box across the aqueous solution phase. This effect also determines critically the formation of the slab. These two combined effects dominate the formation of a CO_2 hydrate slab when using the MI-G methodology, as it occurs with the MI-H technique.[41] Due to the above, the simulation lengths needed for observing induction periods in a proper manner, to distinguish different behaviors of n_h, as a function of time, and the prediction of reliable CO_2 hydrate–water interfacial free energies are much longer compared with those used for simpler systems.

Although the MI-G and MI-H methodologies are similar techniques that allow the estimation of interfacial free energies of hydrates from independent routes, there is an important difference between both methods: In the MI-G technique, we use a mold of associating wells located at the crystallographic equilibrium positions of the guest molecules of the hydrate, i.e., the positions of the carbon atoms of the CO_2 molecules in the sI hydrate structure. However, there exist other subtle but key differences that must be taken into account properly. In the particular case studied in this paper, the number of wells in the mold is lower than that used in the previous work of Algaba *et al.*[41] (they used 56 wells for water molecules and here we use 16 wells for CO_2 molecules, a factor of 3.5 lower). In addition to that, the concentration of CO_2 in the aqueous solution is much lower than that of water in the solution. Particularly, the molar fraction of CO_2 and water in the aqueous solution of CO_2 (one of the phases that coexist at the dissociation line of the CO_2 hydrate at 287 K and 40 MPa) is $x_{CO_2} \approx 0.057$ and $x_{H_2O} \approx 0.943$, respectively. In terms of the number of molecules,

the number of CO_2 and water molecules in the water-rich aqueous phase is $N_{CO_2} \approx 25$ and $N_{H_2O} \approx 380$, respectively. In other words, the factor between the number of water and CO_2 molecules is larger than 15.

The combination of the factors mentioned above produces an effect not observed in either the original MI methodology nor in the MI–H technique. This issue is key in order to identify the induction period and, consequently, the value of the optimal well radius r_w^0. The filling of the wells of the mold used in both, the original MI and MI-H methods, is nearly instantaneous. Usually, all the associating wells of the mold used in these methods are filled typically in ~100 – 200 ps or even less. This is possible (and expected) because a large number of water molecules are available in the center of the simulation box for occupying the associating wells of the mold; in the case of the original MI method, only water molecules exist in the fluid, and in the case of the MI-H method, the composition of water is nearly one ($x_{H_2O} \approx 0.943$), i.e., there are 15 water molecules per CO_2 molecule. However, the situation in the case of the MI-G method is different. It is necessary that there exists a non-negligible period of time, which we have called the filling period, in which the associating wells of the mold used in the MI-G method are occupied by CO_2 molecules.

Figure 4 shows the number of water molecules in the CO_2 hydrate phase, n_h, as a function of time for a well radius $r_w = 0.633$ Å (0.20σ). Here, $\sigma = 3.1668$ Å is the diameter associated with the Lennard-Jones intermolecular potential of the TIP4P/ice model of water used in this work.[42] As we will see later, this election of r_w corresponds to a system in which no induction period exists, i.e., it represents a state in which there is no free energy barrier between the aqueous solution and the incipient hydrate slab (see Fig. 5 and the corresponding explanation in the text for further details and the work of Algaba *et al.*[41]). Consequently, $n_h = n_h(t)$ should grow, on average, monotonically from $t \approx 0$ ns without showing an induction period. However, there exists a period of time, between 0 and ~15.6 ns (red curve in the figure), in which n_h does not behave like this. This time is much larger than the characteristic time in which wells of the molds are occupied in the MI and MI-H methods. What is the reason for this anomalous behavior?

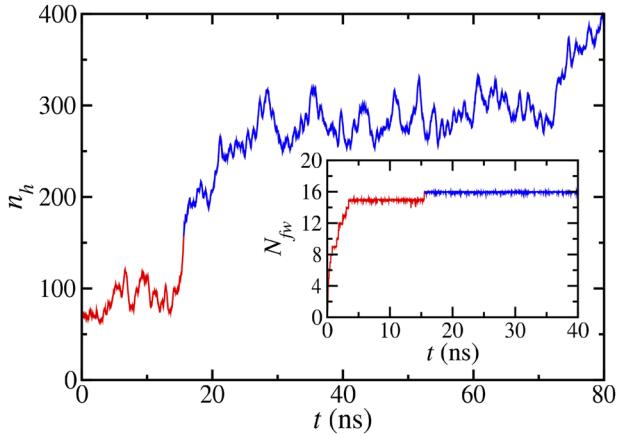

FIG. 4. Number of water molecules in the crystal slab, n_h, as a function of time for a MD trajectory using a well radius $r_w = 0.602$ Å and $\varepsilon = 12k_BT$. The inset represents the number of wells filled with CO_2 molecules as a function of time for the same trajectory. The simulation is performed at coexistence conditions (40 MPa and 287 K). Red curves represent the portion of the trajectory in which not all the wells of the mold are filled and the blue curves the rest of the states in which the mold is fully occupied by CO_2 molecules.

In order to clarify this point, we have also shown the number of wells occupied by CO_2 molecules, N_{fw}, as a function of time in the inset of the figure. As can be seen, for $0 \leq t \lesssim 15.6$ ns (also the red curve in the inset), the wells of the mold are not fully occupied, as it happens for longer simulation times (although in the inset, it seems that the number of wells occupied is sometimes greater than 16, we have checked that this is not the case; it is only a visual effect due to the size employed in the graphical software to show the blue curve appropriately). This behavior is explained in terms of the reduced number of wells as well as the small number of CO_2 molecules, compared with the number of water molecules used in the MI and MI-H techniques. It is important to mention that we have observed filling periods of several nanoseconds for other trajectories and values of r_w. These values are even one order of magnitude larger than those observed in the MI and MI-H methodologies, in which all the molds are usually filled by water molecules in 100–200 ps approximately. Note that the filling period can be confused with the induction period, provoking an erroneous estimation of the optimal well radius, r_w^0, and, consequently, of the interfacial energy of the CO_2 hydrate–water interface. In this particular case, an inspection of the figure without taking into account this issue can cause one to think that this value of r_w (0.602 Å) would correspond to a situation in which there is a free energy barrier between the fluid and the incipient hydrate slab. To avoid this problem, we have identified the filling periods for all the r_w values used in this work and removed them for the evolution of n_h as a function of time. By doing this, we ensure that any period of time from $t \approx 0$ ns is due only to the presence of a free energy barrier or to diffusion time of CO_2 molecules from the borders of the simulation box to the center.

It is important to emphasize that the simulation and thermodynamic conditions used for the MI-H and MI-G techniques are the same. Hence, the diffusion time of CO_2 is the same in both methods. To sum up, once the CO_2 molecules occupy the wells of the mold, the behavior of the system in the MI-G method is identical to that of the MI-H. Particularly, diffusion times and equilibration times are similar in both methods. It would be interesting to study if the diffusion of the guest molecules affects the occupancies of the cages in the MI-H and MI-G methods, but this is beyond the scope of this work.

We have analyzed the time evolution of n_h, the number of water molecules in the CO_2 hydrate slab, for different well radii to obtain a full picture of the behavior of the system according to the discussion in previous paragraphs. We have explored 25 different r_w values, from 0.507 (0.16) to 1.267 Å (0.40σ). Figure 5 shows the evolution of n_h, as a function of time, for a selection of r_w values. According to the previous discussion, we have removed the data corresponding to the number of water molecules in the hydrate phase in all the trajectories for the evolution of $n_h = n_h(t)$. Note that some of the trajectories shown in the figure do not start strictly at $t \approx 0$ ns due to this. The complete set of results is presented in the supplementary material. Particularly, we have carried out several independent

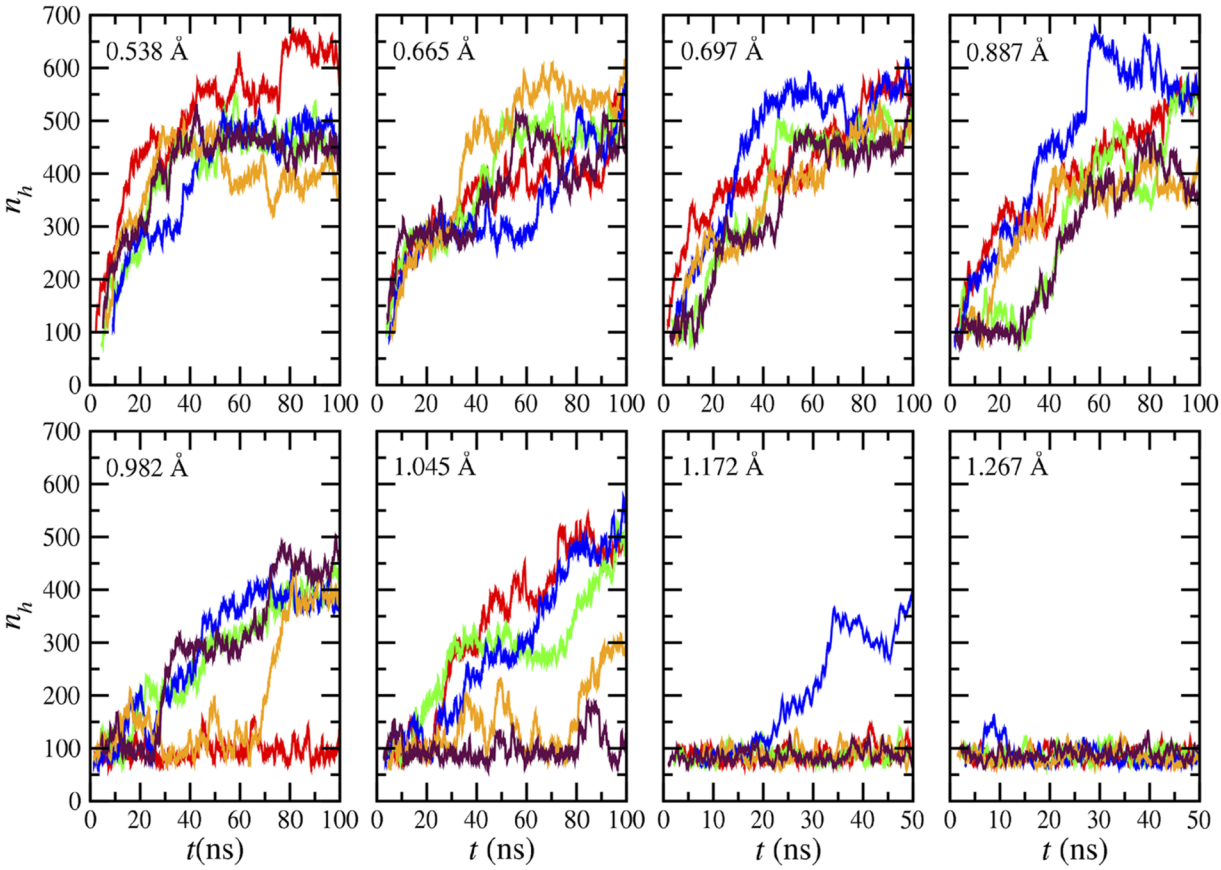

FIG. 5. Number of water molecules in the hydrate slab, n_h, as a function of time for several trajectories and different well radii r_w (as indicated in the legend). All simulations are performed at coexistence conditions (40 MPa and 287 K). In all cases, $\varepsilon = 12k_BT$. Each color represents an independent trajectory generated using different seeds starting from the same fluid configuration.

$NP_z\mathscr{A}T$ simulations starting always with the same configuration. The mold is fully switched on at $\varepsilon = \varepsilon_m = 12k_BT$ in each run and only the well width r_w changes in the range of 0.507–1.267 Å. Simulation lengths used to obtain the correct picture of $n_h = n_h(t)$ are larger than those used by Espinosa and co-workers.[16,36] This is due to the low solubility of CO_2 in water (thermodynamic hindrace) and to the slow diffusion times of CO_2 across the H_2O-rich liquid phase (kinetic hindrance). Particularly, we run each trajectory for 100 ns, which corresponds to the same simulation time used in our previous work using the MI-H methodology to determine the interfacial free energy of the same hydrate.[41]

The evolution of n_h, as a function of time, exhibits different behaviors depending on the r_w value used to analyze how the number of water molecules in the hydrate phase varies with time. Note, as we have mentioned previously, that any possible filling period has been eliminated from all the trajectories shown in Fig. 5 and in the supplementary material. According to this, it is possible to identify three different scenarios: (a) In scenario I, none of the trajectories shows an induction period. This implies, as we have previously mentioned, that the system always crystallizes if simulations are run for enough time. This occurs because there is no free energy barrier between the fluid and hydrate phases in coexistence, which is identified with low values of r_w. (b) In scenario II, at least one trajectory exhibits an induction period. In some cases, the system crystallizes if simulation runs are sufficiently long. However, in other cases, the system does not crystallize even if simulation time is very large ($t < 100$ ns). This behavior is not seen when the original MI technique is used (see Fig. 4 of our previous work.[41]) According to this, there is a free energy barrier low enough that allows the system, in some trajectories, to overcome it and crystallize. This occurs for intermediate values of r_w. (c) In scenario III, all the trajectories show an approximately constant evolution, on average, of n_h with time. In this case, there is a free energy barrier high enough that avoids system crystallization, which corresponds to high values of r_w.

According to the previous discussion, none of the trajectories simulated with $r_w \leq 0.665$ Å (0.21σ) shows an induction period. There is no free energy barrier between the aqueous solution of CO_2 and the thin crystal slab of CO_2 hydrate since n_h grows monotonically from $t \approx 0$ ns, approximately. Care must be taken with these trajectories since the integration path from $\varepsilon = 0$ to $\varepsilon = \varepsilon_m$ crosses a first-order phase transition, and consequently, no

thermodynamic integration is allowed in this case (scenario I). Scenario II is represented by simulations performed with 0.697 Å $\leq r_w \leq$ 1.172 Å ($0.22\sigma \leq r_w \leq 0.37\sigma$). As can be seen, there is at least one trajectory that exhibits an induction period, which means that n_h does not grow, on average, immediately for $t \approx 0$ ns. This behavior, which is also observed when the original MI methodology is applied for pure water and other simplified models,[16,36,58] is also present when the MI-H technique is used to predict interfacial energies of CO_2 hydrates.[41] This corroborates that the systems with this range of values present an energy barrier between the liquid and hydrate phases that avoids the formation of a solid phase irreversibly. In most cases, the system is able to overcome this energetic barrier and form a stable solid phase in the simulation box after some time. However, the MI-G technique reveals a new behavior of the trajectories of $n_h = n_h(t)$ in scenario II. In a few cases (r_w = 0.982, 1.013, 1.045, and 1,172 Å), some trajectories show a different behavior; n_h does not increase with time during the period of time considered in this work (100 ns). In other words, the free energy barrier does not allow the system to develop a complete solid phase. We think this behavior is a consequence of the intrinsic nature of the MI-G methodology. Particularly, the number of associating sites used for the well is low, which implies that the probability of a CO_2 molecule to find one of these elements of the mold is smaller than in the case of the MI-H technique, where the number of sites is 3.5 times larger than in this work. Finally, all trajectories considered for systems with $r_w \geq 1.267$ Å (0.40σ) show the same behavior: n_h, as a function of t, remains approximately constant due to the presence of an energy barrier between the solid phase and the aqueous solution of CO_2 that avoids system crystallization. It is also important to mention that for $r_w \geq 1.425$ Å (0.45σ), we have observed multiple filling of the well sites, which represents an upper limit of well radius that can be used to calculate ΔG_m with consistency.

Following the previous studies,[16,36,41] r_w^0 is located between r_w = 0.665 Å (0.21σ) and r_w = 0.697 Å (0.22σ). As in the case of the MI-H methodology, the MI-G technique also suffers from thermodynamic and kinetic hindrances, making it difficult to establish the precise optimal value r_w^0 for calculating the correct interfacial energy value. Following our previous work, it is necessary to provide enough uncertainty to ensure that r_w^0 as well as γ_{hw} is given in the appropriate confidence interval. We assume that the lower and upper bounds for r_w^0 are $r_w^{(l)}$ = 0.554 Å (0.175σ) and $r_w^{(u)}$ = 0.808 Å (0.255σ), respectively. This election implies $r_w^0 = \frac{r_w^{(l)} + r_w^{(u)}}{2} \approx 0.681$ Å, which corresponds to a mean value of the upper and lower bounds of r_w^0. The uncertainty of r_w^0 is estimated to be equal to one half of the difference between $r_w^{(l)}$ and $r_w^{(u)}$, $\sigma_{r_w^0} = \frac{r_w^{(u)} - r_w^{(l)}}{2} \approx 0.127$ Å. The optimal value with a conservative confidence interval is then $r_w^0 = 0.68(13)$ Å.

D. Thermodynamic integration

Following the methodology of the original MI and the MI-H techniques, the next step is to determine the interfacial free energy for systems in which the mold interaction width, r_w, is greater than the optimal one, i.e., $r_w > r_w^0$. The selected values to perform the thermodynamic integration, given by Eq. (3), are r_w = 1.140, 1.172, 1.203, 1.235, and 1.267 Å.

Calculation of γ_{hw} for each r_w requires the knowledge of the average filled wells with CO_2 molecules, $\langle N_{fw} \rangle_{NP_z\mathscr{A}T}$, for a given number of ε values. Typically, we perform MD simulations in the $NP_z\mathscr{A}T$ ensemble for 20 different values of ε, between $\varepsilon = 0$ and $\varepsilon = \varepsilon_m = 12k_BT$. Each point has been obtained by starting the simulations from the initial fluid configuration and switching the mold on with the corresponding well–water interaction parameter ε. Simulations are equilibrated during 10 ns and $N_{fw}(\varepsilon)$, the number of filled wells, is averaged over 40 ns. Uncertainties are estimated using the well-known sub-block method. The production period, 40 ns, is divided into M independent blocks. The statistical errors are then estimated from the standard deviation of the average, $\sigma_{\langle N_{fw} \rangle} = \overline{\sigma}_{fw}/\sqrt{M}$, where $\overline{\sigma}_{fw}$ is the variance of block average and M has been fixed to $M = 10$.

A typical profile of $\langle N_{fw} \rangle_{NP_z\mathscr{A}T}$, as a function of ε, is sketched in Fig. 6. Note that we have also fit the MD simulation results obtained to a hyperbolic tangent continuous function. This is done to smooth the results obtained using Eq. (3) for the integration of $\langle N_{fw} \rangle_{NP_z\mathscr{A}T}$ and the determination of ΔG^{hw}. We have also included an inset in Fig. 6 that shows the fit of all the mold interaction widths used in this work. Notice the slight deviation among the curves, corresponding to the use of different values of r_w. As can be seen, when the well–CO_2 interaction is turned off, there is a minimum occupancy of about 0.2. As ε increases to the maximum value, the average number of filled wells also increases smoothly, showing a plateau that corresponds to states in which only one CO_2 molecule occupies each of the wells. The maximum value used in this work, $\varepsilon_m = 12k_BT$, satisfies the conditions that ensure the appropriateness of the technique:[16,41] (1) Every well of the mold is occupied by only one CO_2 molecule in the final state of the thermodynamic integration, i.e., $\langle N_{fw} \rangle_{NP_z\mathscr{A}T} \to N_w$ when $\varepsilon \to \varepsilon_m$; and (2) $\varepsilon_m = 12k_BT$ ensures the smoothness of $\langle N_{fw} \rangle_{NP_z\mathscr{A}T}$ as a function of ε. As in

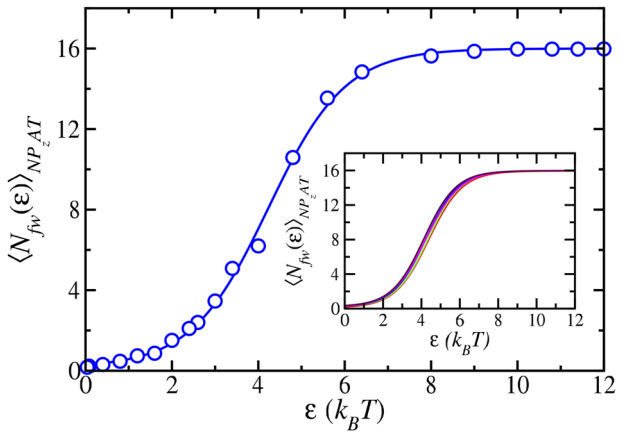

FIG. 6. Average number of filled wells, $\langle N_{fw}(\varepsilon) \rangle_{NP_z\mathscr{A}T}$, as a function of the well depth ε, for the principal plane of the CO_2 hydrate. The radius of the mold used is r_w = 1.235 Å. The circles correspond to the values obtained from $NP_z\mathscr{A}T$ simulations of 40 ns and the blue curve represents its corresponding fit. The inset represents the fits of the average number of filled wells using well radii higher than the optimal value, r_w = 1.140 (red), 1.172 (green), 1.203 (blue), 1.235 (magenta), and 1.267 Å (maroon).

TABLE II. Free energy change, ΔG_m, and CO_2 hydrate–water interfacial free energy, γ_{hw}, at coexistence conditions (40 MPa and 287 K), as functions of the well radius $r_w > r_w^0$. Results have been obtained from MD simulations using a mold of wells switched on with well energy $\varepsilon = 12k_BT$ and $r_w > r_w^0$.

r_w (Å)	ΔG_m (k_BT)	γ_{hw} (mJ/m^2)
1.140	121.82	24.06
1.172	123.10	23.63
1.203	125.01	22.97
1.235	124.84	23.03
1.267	126.56	22.44

the work of Algaba *et al.*,[41] we have checked that other values of ε_m provide the same curve as that shown in Fig. 6.

It is important to mention here that the states visited by the system along all the trajectories used to determine ΔG^{hw}, for different r_w and ε values, correspond to liquid states. This ensures that the integration path chosen from $\varepsilon = 0$ to ε_m does not cross a first-order transition. According to our previous work (see Fig. 6 and the corresponding explanation in the text of the work of Algaba *et al.*[41] for further details), this can be confirmed by inspecting the number of water molecules that belong to the hydrate slab, n_h, and checking that it does not grow for any ε value. Inspection of Fig. 6 and the supplementary material indicates that this does not happen for $\varepsilon = \varepsilon_m$. Although it is not shown here, we have checked that the same is true for $0 < \varepsilon < \varepsilon_m$ and all the r_w values used in this work for the thermodynamic integration. This confirms that ΔG_m can be directly related to ΔG^{hw}, and, consequently, that it is possible to obtain reliable values of γ^{hw}. Table II shows the free energy changes ΔG_m, due to the perturbation energy inserted by the mold, for each well radius r_w. Combining these results with Eqs. (1) and (4), it is possible to obtain the CO_2 hydrate–water interfacial free energy for well radius greater than the optimal value ($r_w > r_w^0$).

It is important to take into account the following issue. In this work, we have assumed that the cage occupancy in the hydrate is near full and it could be different from unity. In fact, it is estimated experimentally that occupancy is usually in the range 80%–100%. According to our previous investigations on the effect of occupancy on the dissociation line of the CO_2 hydrate,[38] occupancy above 75% does not modify the position of the line. However, the effect of occupancy on the interfacial free energy is currently unknown. It would be interesting to analyze the effect of occupancy of this magnitude using the MI methodology but it seems to be a nontrivial problem. In principle, the interfacial free energy of the hydrate calculated using the MI-G (and also the MI-H) method would depend only on the occupancy of the thin slab of hydrate induced close to the wells of the mold. Unfortunately, this goal is beyond the scope of this work and deserves a complementary study in a future work.

E. CO_2 hydrate–water interfacial free energy

Once the CO_2 hydrate–water interfacial free energy is obtained for different values of $r_w > r_w^0$, it is possible to determine the real value of γ_{hw}. Following the approach proposed in previous studies,[16,36,41] we represent the interfacial energy vs r_w. As can be seen in Fig. 7, γ_{hw} behaves as a linear function of r_w. This is in agreement with previous results and confirms that the interfacial free energy of the CO_2 hydrate–water interface obtained from the MI-G methodology follows the same linear trend with r_w.

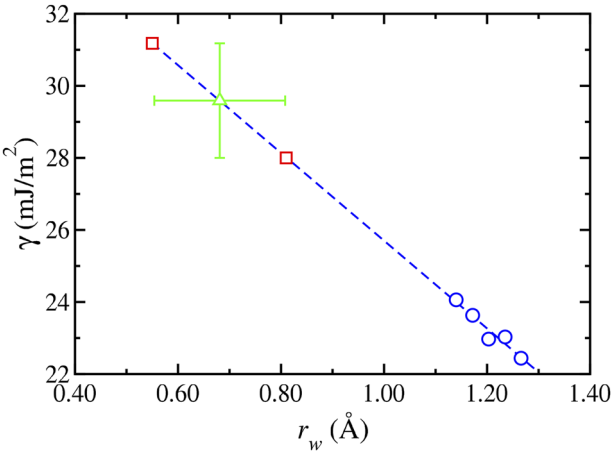

FIG. 7. CO_2 hydrate–water interfacial free energy as a function of the potential well radius of the mold as obtained from the MI-G methodology (open blue circles). The dashed line represents a linear fit of the data, the open red squares the interfacial tension evaluated at $r_w^{(l)}$ and $r_w^{(u)}$, and the open green diamond the extrapolation of the linear fit to the optimal well radius.

To determine the interfacial free energy, we perform a linear fit of the MD simulation data and estimate the value of γ_{hw} evaluated at $r_w = r_w^0 = 0.68(13)$ Å, which corresponds with the mean value of the interfacial energy at the lower and upper bounds of r_w, $r_w^{(l)} = 0.55$ Å ($\gamma_{hw}^{(l)} = 31.18$ mJ/m^2) and $r_w^{(u)} = 0.81$ Å ($\gamma_{hw}^{(u)} = 28.00$ mJ/m^2), both obtained in Sec. IV C. The values of the interfacial energy at the lower and bound limits of the well radius are shown in Fig. 7 as open red squares, and the estimation of the CO_2 hydrate–water interfacial energy at r_w^0 is represented as an open green diamond ($\gamma_{hw} = 29.59$ Å).

To estimate the uncertainty associated with this value, we follow the procedure used in our previous work[41] and assume that the main source of error in γ_{hw} comes from the uncertainty due to r_w^0. Under these conditions and since the value of γ_{hw} is located at the middle of the interval $[\gamma_{hw}^{(l)}, \gamma_{hw}^{(u)}]$, the error associated with γ_{hw} is $\sigma_{\gamma_{hw}} = (\gamma_{hw}^{(u)} - \gamma_{hw}^{(l)})/2 \approx 1.59$ mJ/m^2. With this election, $\gamma_{hw} = 30(2)$ mJ/m^2 (see open green diamond).

It is interesting to compare the predictions obtained from the MI-G methodology with experimental data taken from the literature. As mentioned in the Introduction, only Uchida *et al.*[17,18] and Anderson and co-workers[19,20] have published (indirect) experimental data. The value obtained in this work, 30(2) mJ/m^2, is in good agreement with experiments of Uchida *et al.*, 28(6) mJ/m^2, and also in excellent agreement with data from the work of Anderson *et al.*, 30(3) mJ/m^2. The results obtained in this work are based on the thermodynamic definition of the interfacial free energy between the CO_2 hydrate and the aqueous solution of CO_2 in contact with it, the use of realistic molecular models for water (TIP4P/ice) and CO_2 (TraPPE), the use of the well-established MD technique, and

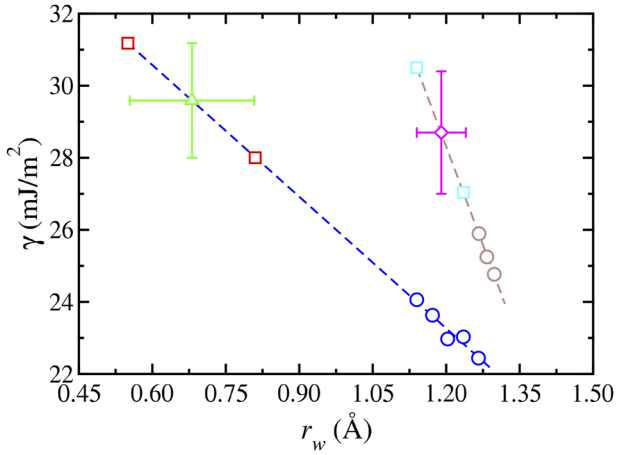

FIG. 8. CO_2 hydrate–water interfacial free energy as a function of the potential well radius of the mold as obtained from the MI-G (open blue circles) and the MI-H (open brown circles) methodologies. The blue dashed (MI-G) and brown dashed (MI-H) lines represent linear fits of the data, the open red (MI-G) and open turquoise (MI-H) squares the interfacial tension evaluated at $r_w^{(l)}$ and $r_w^{(u)}$ in both methodologies, and the open green (MI-G) and open magenta (MI-H) diamonds the extrapolation of the linear fit to the optimal well radius in both methodologies.

information obtained from standard rotationally invariant local bond order parameters. Consequently, one of the main results of this work is that TIP4P/ice and TraPPE are good models for predicting interfacial free energies of CO_2 hydrates according to the results obtained from the use of the MI-G methodology and their agreement with experimental data taken from the literature.

Although agreement with experimental data is important, it is also relevant to check the internal consistency of the mold integration method and compare predictions obtained using the MI-G and MI-H methodologies. To this end, Fig. 8 shows the behavior of the CO_2 hydrate interfacial free energy using both techniques. According to our previous calculations (MI-H), the CO_2 hydrate–water interfacial free energy is 29(2) mJ/m^2. Our new estimate of the interfacial free energy (MI-G) is 30(2) mJ/m^2, which is in excellent agreement with the prediction from the MI-H method.

Although both methods are based on the mold integration method proposed by Espinosa and co-workers,[36] it is important to emphasize that both routes are completely independent calculations. In the case of the work of Algaba and co-workers, the MI-H technique uses a mold of associating wells, located in the crystallographic equilibrium positions occupied by the oxygen of atoms of water molecules in a principal plane of the sI hydrate. Particularly, they used $N_w = 56$ wells, with an optimal interaction range $r_w^0 = 1.19(5)$ Å and a maximum well depth $\varepsilon_m = 8k_BT$. In the current work, we introduce the MI-G method, which comprises a mold of associating wells located at the center of the cages T and D of the sI hydrate structure, the equilibrium positions occupied by the carbon atoms of the CO_2 molecules in two different planes. Here, we use only $N_w = 16$ wells, with an optimal interaction range $r_w^0 = 0.68(13)$ Å, and a maximum well depth $\varepsilon_m = 12k_BT$. Obviously, due to the nature and characteristics of the different molds used in both cases, the results obtained can be considered independent.

It is also interesting to note that the range of r_w values used to estimate γ_{hw} as well as the (negative) slope of the linear fitting of γ_{hw} with r_w are different in each methodology. Particularly, the variation of the interfacial free energy with the well radius is higher in the case of the MI-H method. This is expected since in the MI-H technique, a larger number of associating wells is used ($N_w = 56$) compared with those employed in the MI-G methodology ($N_w = 16$). The upper and lower bounds of the r_w values used to estimate γ_{hw} at coexistence are also different in both techniques. However, the value for γ_{hw} provided by both techniques is the same within the corresponding error bars.

Taking into account the above discussion, the results obtained here are highly relevant to the scientific community of hydrates. The mold integration methodology and the two particular versions developed to deal with the prediction of the interfacial free energy of hydrates open new possibilities for predicting this magnitude for complex solid phases, including other hydrates. We think the complementary use of both methods to check the consistency of results obtained is a good strategy to determine the interfacial energies of these systems.

V. CONCLUSIONS

We have calculated the CO_2 hydrate–water interfacial free energy from MD computer simulations. We use the well-known TraPPE (CO_2) and TIP4P/ice (H_2O) molecular models that are able to predict accurately the thermodynamic conditions at which the dissociation line of the CO_2 hydrate occurs as well as the interfacial energy of the ice–water interface. The calculations, which are performed at coexistence conditions, are based on the definition of the interfacial free energy and the use of well-established tools from thermodynamics and statistical mechanics.

In a previous paper, we extended the original Mold Integration (MI) methodology to account for CO_2 hydrates, which implies to deal with binary mixtures that exhibit liquid–liquid immiscibility, instead of a pure fluid, and to optimize local-order parameters to identify water-like and hydrate-like particles in these systems. According to the method, the interfacial energy is evaluated using a mold of attractive sites occupying the crystallographic equilibrium positions of a layer of oxygen atoms of water molecules in the CO_2 hydrate to induce reversibly the formation of a hydrate slab.

In this work, we take a step forward and propose the use of a mold of attractive sites located at the crystallographic equilibrium positions of a layer of carbon atoms of CO_2 molecules in the CO_2 hydrate. The main advantages of the new technique, which we call Mold Integration–Guest (MI-G) method, over the original methodology are twofold: (1) The number of attractive sites forming the mold to induce the formation of the hydrate is lower; and (2) the information needed to build the mold is also much less since only 8 CO_2 molecules vs the 46 water molecules exist in a hydrate unit cell.

We use the MI-G technique, with the appropriate parameters that characterize the associating sites of the mold, to obtain the interfacial free energy of the CO_2 hydrate. The results obtained clearly show that the new methodology is able to induce the formation of slabs of CO_2 hydrates with information on the equilibrium crystallographic position of the CO_2 molecules alone. This is particularly remarkable since no information for the equilibrium positions of

water in the slab hydrate is provided. Calculations are compared with the only two indirect experimental measurements existing in the literature, from the work of Uchida *et al.* and that of Anderson and co-workers. In addition, we also compare the predictions made by the MI-G method with the results obtained previously using the original MI implementation.

The interfacial free energy value obtained in this work agrees very well with that obtained in previous calculations using the MI-H technique. The agreement between theoretical calculations and experimental values of Uchida and Anderson is also remarkable. According to the results presented here, the TIP4P/ice and TraPPE models for water and CO_2 molecules, respectively, and the MI methodology can be considered as a valuable complementary and alternative approach to provide interfacial free energies of CO_2 hydrates.

SUPPLEMENTARY MATERIAL

See the supplementary material for the time evolution of the number of water molecules in the CO_2 hydrate slab for the 25 different well radii considered and also for the multimedia results (movies) obtained from MD computer simulations using the MI-H and MI-G techniques showing crystallization and no crystallization starting from an equilibrated liquid–liquid configuration of the $CO_2 + H_2O$ binary mixture.

ACKNOWLEDGMENTS

We thank Jorge R. Espinosa, E. Sanz, and Carlos Vega for helpful discussions and Centro de Supercomputación de Galicia (CESGA, Santiago de Compostela, Spain) for providing access to computing facilities. We also acknowledge financial support from Ministerio de Ciencia e Innovación (Grant No. PID2021-125081NB-I00), Junta de Andalucía (Grant No. P20-00363), and Universidad de Huelva (Grant Nos. P.O. FEDER UHU-1255522 and FEDER-UHU-202034), all four co-financed by EU FEDER funds.

AUTHOR DECLARATIONS

Conflict of Interest

The authors have no conflicts to disclose.

Author Contributions

Iván M. Zerón: Conceptualization (equal); Formal analysis (equal); Funding acquisition (equal); Visualization (lead); Writing – original draft (lead); Writing – review & editing (equal). **José Manuel Míguez**: Conceptualization (equal); Validation (equal). **Bruno Mendiboure**: Formal analysis (lead); Methodology (lead). **Jesús Algaba**: Formal analysis (equal); Investigation (equal); Methodology (equal); Visualization (lead); Writing – original draft (lead). **Felipe J. Blas**: Conceptualization (equal); Funding acquisition (equal); Investigation (equal); Methodology (equal); Writing – review & editing (equal).

DATA AVAILABILITY

The data that support the findings of this study are available from the corresponding author upon reasonable request.

REFERENCES

[1] E. D. Sloan and C. Koh, *Clathrate Hydrates of Natural Gases*, 3rd ed. (CRC Press, New York, 2008).
[2] A. Y. Manakov, S. V. Goryainov, A. V. Kurnosov, A. Y. Likhacheva, Y. A. Dyadin, and E. G. Larionov, J. Phys. Chem. B **107**, 7861 (2003).
[3] T. Makino, T. Sugahara, and K. Ohgaki, J. Chem. Eng. Data **50**, 2058 (2005).
[4] K. A. Kvenvolden, Chem. Geol. **71**, 41 (1988).
[5] C. A. Koh, A. K. Sum, and E. D. Sloan, J. Nat. Gas Sci. Eng. **8**, 132 (2012).
[6] E. D. Sloan, Science **426**, 353 (2003).
[7] M. Yang, Y. Song, L. Jiang, Y. Zhao, X. Ruan, Y. Zhang, and S. Wang, Appl. Energy **116**, 26 (2014).
[8] M. Ricaurte, C. Dicharry, X. Renaud, and J.-P. Torré, Fuel **122**, 206 (2014).
[9] V. Chihaia, S. Adams, and W. F. Kuhs, Chem. Phys. **317**, 208 (2005).
[10] B. Peters, N. E. R. Zimmermann, G. T. Beckham, J. W. Tester, and B. L. Trout, J. Am. Chem. Soc. **130**, 17342 (2008).
[11] N. J. English and J. S. Tse, Phys. Rev. Lett. **103**, 015901 (2009).
[12] P. G. Debenedetti, *Metastable Liquids: Concepts and Principles* (Princeton University Press, 1997).
[13] A. W. Adamson and A. P. Gast, *Physical Chemistry of Surfaces* (John Wiley & Sons, 1997).
[14] R. D. Weir and E. T. W. de Loos, "Chapter 15: Measurement of surface and interfacial tensions," in *Measurement of the Thermodynamic Properties of Multiple Phases*, Experimental Thermodynamics (Elsevier, 2005).
[15] B. H. Alexander, M. H. Dawson, and H. P. Kling, J. Appl. Phys. **22**, 439 (1951).
[16] J. R. Espinosa, C. Vega, and E. Sanz, J. Phys. Chem. C **120**, 8068 (2016).
[17] T. Uchida, T. Ebinuma, and T. Ishizaki, J. Phys. Chem. B **103**, 3659 (1999).
[18] T. Uchida, T. Ebinuma, S. Takeya, J. Nagao, and H. Narita, J. Phys. Chem. B **106**, 820 (2002).
[19] R. Anderson, M. Llamedo, B. Tohidi, and R. W. Burgass, J. Phys. Chem. B **107**, 3500 (2003).
[20] R. Anderson, M. Llamedo, B. Tohidi, and R. W. Burgass, J. Phys. Chem. B **107**, 3507 (2003).
[21] Y. Seo, H. Lee, and T. Uchida, Langmuir **18**, 9164 (2002).
[22] W. Zhang, J. W. Wilder, and D. H. Smith, J. Phys. Chem. B **107**, 13084 (2003).
[23] D. H. Smith, J. W. Wilder, and K. Seshadri, AIChE J. **48**, 393 (2002).
[24] D. H. Smith, K. Seshadri, T. Uchida, and J. W. Wilder, AIChE J. **50**, 1589 (2004).
[25] S.-P. Kang, J.-W. Lee, and H.-J. Ryu, Fluid Phase Equilib. **274**, 68 (2008).
[26] Y. Zhang, X.-S. Li, Y. Wang, Z.-Y. Chen, and K.-F. Yan, Fluid Phase Equilib. **413**, 110 (2016).
[27] H. Liu, S. Zhan, P. Guo, S. Fan, and S. Zhang, Chem. Eng. J. **349**, 775 (2018).
[28] M. Zarifi, J. Javanmardi, H. Hashemi, A. Eslamimanesh, and A. H. Mohammadi, Fluid Phase Equilib. **423**, 17 (2016).
[29] A. Phan, H. M. Stoner, M. Stamatakis, C. A. Koh, and A. Striolo, J. Colloid Interface Sci. **611**, 421 (2022).
[30] L. C. Jacobson, W. Hujo, and V. Molinero, J. Am. Chem. Soc. **132**, 11806 (2010).
[31] L. C. Jacobson, W. Hujo, and V. Molinero, J. Phys. Chem. B **114**, 13796 (2010).
[32] J. Q. Broughton and G. H. Gilmer, J. Chem. Phys. **84**, 5759 (1986).
[33] J. J. Hoyt, M. Asta, and A. Karma, Phys. Rev. Lett. **86**, 5530 (2001).
[34] S. Angioletti-Uberti, M. Ceriotti, P. D. Lee, and M. W. Finnis, Phys. Rev. B **81**, 125416 (2010).
[35] L. A. Fernández, V. Martín-Mayor, B. Seoane, and P. Verrocchio, Phys. Rev. Lett. **108**, 165701 (2012).
[36] J. R. Espinosa, C. Vega, and E. Sanz, J. Chem. Phys. **141**, 134709 (2014).
[37] Z. M. Aman and C. A. Koh, Chem. Soc. Rev. **45**, 1678 (2016).
[38] J. M. Míguez, M. M. Conde, J.-P. Torré, F. J. Blas, M. M. Piñeiro, and C. Vega, J. Chem. Phys. **142**, 124505 (2015).

[39]J. Costandy, V. K. Michalis, I. N. Tsimpanogiannis, A. K. Stubos, and I. G. Economou, J. Chem. Phys. **143**, 094506 (2015).
[40]M. H. Waage, T. J. H. Vlugt, and S. Kjelstrup, J. Phys. Chem. B **121**, 7336 (2017).
[41]J. Algaba, E. Acuña, J. M. Míguez, B. Mendiboure, I. M. Zerón, and F. J. Blas, J. Colloid Interface Sci. **623**, 354 (2022).
[42]J. L. F. Abascal, E. Sanz, R. García Fernández, and C. Vega, J. Chem. Phys. **122**, 234511 (2005).
[43]J. J. Potoff and J. I. Siepmann, AIChE J. **47**, 1676 (2001).
[44]W. Lechner and C. Dellago, J. Chem. Phys. **129**, 114707 (2008).
[45]R. Radhakrishnan and B. L. Trout, J. Chem. Phys. **117**, 1786 (2002).
[46]S. Hirai, K. Okazaki, Y. Tabe, and K. Kawamura, Energy Convers. Manage. **38**, S301 (1997).
[47]E. Sanz, C. Vega, J. R. Espinosa, R. Caballero-Bernal, J. L. F. Abascal, and C. Valeriani, J. Am. Chem. Soc. **135**, 15008 (2013).
[48]M. P. Allen and D. J. Tildesley, *Computer Simulation of Liquids*, 2nd ed. (Oxford University Press; Clarendon, Oxford, 2017).
[49]D. Frenkel and B. Smit, *Understanding Molecular Simulations*, 2nd ed. (Academic, San Diego, 2002).
[50]E. G. Noya, C. Vega, and E. de Miguel, J. Chem. Phys. **128**, 154507 (2008).
[51]D. Frenkel, Eur. Phys. J. Plus **128**, 10 (2013).
[52]J. R. Espinosa, E. Sanz, C. Valeriani, and C. Vega, J. Chem. Phys. **139**, 144502 (2013).
[53]M. A. Cuendet and W. F. V. Gunsteren, J. Chem. Phys. **127**, 184102 (2007).
[54]S. Nosé, Mol. Phys. **52**, 255 (1984).
[55]M. Parrinello and A. Rahman, J. Appl. Phys. **52**, 7182 (1981).
[56]U. Essmann, L. Perera, M. L. Berkowitz, T. Darden, H. Lee, and L. G. Pedersen, J. Chem. Phys. **103**, 8577 (1995).
[57]J. M. Míguez, M. M. Piñeiro, J. Algaba, B. Mendiboure, J. P. Torré, and F. J. Blas, J. Phys. Chem. B **119**, 14288 (2015).
[58]J. R. Espinosa, C. Vega, C. Valeriani, and E. Sanz, J. Chem. Phys. **142**, 194709 (2015).
[59]T. M. Truskett, S. Torquato, and P. G. Debenedetti, Phys. Rev. E **62**, 993 (2000).
[60]P.-L. Chau and A. J. Hardwick, Mol. Phys. **93**, 511 (1998).
[61]J. S. van Duijneveldt and D. Frenkel, J. Chem. Phys. **96**, 4655 (1992).
[62]P. R. ten Wolde, M. J. Ruiz-Montero, and D. Frenkel, Phys. Rev. Lett. **75**, 2714 (1995).
[63]R. M. Lynden-Bell, J. S. van Duijneveldt, and D. Frenkel, Mol. Phys. **80**, 801 (1993).
[64]P. Rein ten Wolde, M. J. Ruiz-Montero, and D. Frenkel, J. Chem. Phys. **104**, 9932 (1996).